Journal of Solid State Chemistry 182 (2009) 1088–1093

Contents lists available at ScienceDirect

Journal of Solid State Chemistry

journal homepage: www.elsevier.com/locate/jssc

CTAB-assisted synthesis and photocatalytic property of CuO hollow microspheres

Shunli Wang, Hui Xu, Liuqin Qian, Xi Jia, Junwei Wang, Yangyi Liu, Weihua Tang *

Department of Physics, Center for Optoelectronics Materials and Devices, Zhejiang Sci-Tech University, Hangzhou, Zhejiang 310018, PR China

ARTICLE INFO

Article history:
Received 22 October 2008
Received in revised form
14 January 2009
Accepted 26 January 2009
Available online 12 February 2009

Keywords:
CuO
Synthesis
Hollow microsphere
Photocatalytic property

ABSTRACT

CuO hollow microspheres have been fabricated through a simple hydrothermal method in the presence of cetyltrimethylammonium bromide (CTAB). The products were characterized by Fourier transform infrared spectroscopy, X-ray diffraction, and scanning electron microscopy. The effects of reaction temperature, surfactant, and the molar ratio of Urea/Cu(II) on the morphologies of the resulting products were investigated. The possible formation mechanism of CuO hollow dandelion-like architectures was proposed. The hierarchical CuO hollow microspheres exhibited a high photocatalytic activity for decolorization of Rhodamine B (RhB) under UV-light illumination.

1. Introduction

Hierarchical semiconductor structure has been widely exploited for diverse applications such as heterogeneous catalysis, gas sensors, lithium ion electrode materials, magnetic materials, and superconductors [1–5]. Especially, CuO nanostructures with hollow spherical morphology represent useful applications in catalysts, fillers, coatings and encapsulating agents, due to their low density, large specific surface area, and interesting optical properties [6]. Many strategies have been developed for the fabrication of nanomaterials with hollow structures, such as templates [7–9], chemical processes based on differential diffusion (Kirkendall effect) [10,11], Ostwald ripening [12,13], and chemically induced self-transformation [14,15]. Liu and Zeng [16] reported the synthesis of CuO dandelion-like architectures with hollow interiors by the hydrothermal method. Zhang et al. [17] fabricated hollow CuO microspheres on a large scale through a rational complexing reagent-assisted approach at low temperature. Yu et al. [18] prepared CuO/Cu_2O composite hollow microspheres with controlled diameter and composition. Ng and Fan [19] reported the synthesis of CuO with the tetrahedral nanocage morphology by the oxidation of γ-CuI nanotetrahedrons. Qi et al. [20] fabricated CuO nanoparticle interlinked microsphere cages by solution method. CuO has been applied to improve the photocatalytic efficiency of some other semiconductors [21,22], however, little information concerning the photocatalytic activity of pure copper oxide was reported [23].

The electrostatic interactions between surfactant molecules and charged or polarized metal-oxyprecursors have been widely applied to metastable modifications of metal oxides [24–26]. Cetyltrimethylammonium bromide (CTAB) is a cationic surfactant, which can form spherical $C_{16}H_{33}(CH_3)_3N^+$ (CTA^+) micelles [27] and can be employed to synthesize materials with hollow structures. $CaCO_3$ [28], mesoporous silica [29], and $LiAlO_2$ hollow spheres [30] have been prepared with CTAB as the template. In this paper, CTAB-assisted synthesis and photocatalytic activity of dandelion-like CuO hollow microspheres were studied. The formation mechanism of dandelion-like CuO hollow microspheres was proposed. The effects of reaction temperature, surfactant, and the molar ratio of Urea/Cu(II) on the morphologies and phases of the resulting products were investigated. Moreover, the photocatalytic activity of the dandelion-like CuO hollow microspheres was evaluated by examining the degradation of RhB.

2. Experimental

2.1. Sample preparation

All chemical reagents were of analytical grade. In a typical procedure, 2.0 mmol $Cu(NO_3)_2 \cdot 3H_2O$, 6.0 mmol $CO(NH_2)_2$, and 2.7 mmol CTAB were added to distilled water (15 mL) under stirring to form a homogeneous solution. The solution was then transferred into a stainless steel autoclave with a Teflon liner of 20 mL capacity, and heated in an oven at 180 °C for 1, 2, 4, and 6 h,

* Corresponding author. Fax: +86 57186843222.
E-mail address: whtang@zstu.edu.cn (W.H. Tang).

0022-4596/$ - see front matter © 2009 Elsevier Inc. All rights reserved.
doi:10.1016/j.jssc.2009.01.042

respectively. After the autoclave was air-cooled to room temperature, the resulting product was filtered, washed with distilled water and absolute ethanol several times, and then dried under vacuum at 80 °C for 4 h.

2.2. Characterization

The crystallographic information of the prepared samples was analyzed by powder X-ray diffraction (XRD) using a Bruker AXS D8 DISCOVER X-ray diffractometer with Cu$K\alpha$ radiation ($\lambda = 1.5406$ Å) at a scanning rate of 1° min^{-1}. Fourier transform infrared (FT-IR) spectra were measured using the KBr method on a Fourier transform infrared spectrometer (FTIR Nicolet 5700). Each FTIR spectrum was collected after 40 scans at a resolution of 4 cm^{-1} from 400 to 4000 cm^{-1}. Scanning electron microscopy (SEM) images were taken on a JSM-5610LV scanning electron microscope with acceleration voltage of 20 kV.

2.3. Photocatalytic activity test

The photocatalytic activity of the prepared samples was evaluated by the photocatalytic decolorization of RhB aqueous solution performed at room temperature (ca. 25 °C). The experimental procedure was as follows: 10 mg of the prepared powders were dispersed in 20 mL of RhB aqueous solution with a concentration of 2.0×10^{-5} mol L^{-1} in a beaker (with a capacity of 100 mL), and the suspensions were placed in the dark for 30 min before illumination to allow sufficient adsorption of RhB. A UV-light lamp placed 7 cm above the beaker with a wavelength of 254 nm was used as a light source. The concentration of RhB aqueous solution was determined by a UV–visible spectrophotometer (UV-4802H, UNICO). After UV-light irradiation for 10 min, the reaction solution was filtered, and the absorbance of RhB aqueous solution was then measured.

3. Results and discussion

3.1. Crystal structure and morphology of the prepared products

XRD analysis was utilized to analyze the crystal structure and phase composition of the resulting CuO products. Fig. 1 shows the XRD patterns of the samples obtained under different synthetic conditions. Fig. 1a shows the XRD pattern of the precursor obtained by hydrothermal reaction for 1 h in the presence of CTAB. All of the diffraction peaks can be readily indexed to monoclinic phase $Cu_2(OH)_2CO_3$ (JCPDS Card file no. 41-1390). No impurities peak was found. The XRD pattern shown in Fig. 1b is the product obtained by hydrothermal reaction for 2 h in the presence of CTAB. The diffraction peaks can be clearly indexed to both phases with the monoclinic copper hydroxide carbonate (JCPDS Card file no. 41-1390, $Cu_2(OH)_2CO_3$) and the monoclinic copper oxide (JCPDS Card file no. 80-1916, CuO). When the reaction time was extended to 6 h, pure copper oxide was prepared (shown in Fig. 1c), and the diffraction peaks can be indexed to the monoclinic copper oxide (JCPDS Card file no. 80-1916, CuO).

FTIR investigation also confirmed the formation of copper hydroxide carbonate and copper oxide. Figs. 2a and b show the FTIR spectra of the products obtained at 180 °C in the presence of CTAB for 1 and 6 h, respectively. The strong peak at 3406 cm^{-1} is assigned to the stretching vibration of the O–H bond, ν(OH), which indicates the presence of hydroxyl ions due to the metal-OH layer. The peak at 3315 cm^{-1} is attributed to the O–H groups interacting with carbonate anions. The peaks 1511, 1430, 1384, 1095, 1047, 873, 817, and 746 cm^{-1}, and the peaks 572, 524 and 428 cm^{-1} are assigned to CO_3^{2-} and Cu–O, respectively [31]. In addition, the bands 3455 and 1634 cm^{-1} (Fig. 2b) could be attributed to the stretching vibration and bending vibration of the absorbed water and surface hydroxyl groups, respectively. The peaks 596, 528, and 434 cm^{-1} are due to monoclinic phase of CuO [31, p. 220]. No other absorption peaks could be detected.

Fig. 3 shows SEM images of the hierarchical CuO obtained by hydrothermal reaction for 6 h in the presence of CTAB. The CuO is composed of many dandelion-like structures with hollow interior, and the diameters of the CuO microspheres range from 5 to 10 μm. Fig. 3b shows that the "dandelions" have a hollow cavity clearly, and the CuO microspheres are composed of small crystal strips. These crystal strips are aligned perpendicularly to the spherical surface, pointing toward a common center. Fig. 4 shows the SEM images of the products obtained by hydrothermal reaction in the presence of CTAB for 1, 2, 4, and 6 h. The SEM image of Fig. 4a indicates that the product is composed of many small ribbons. In accordance with the XRD results, the ribbons are of monoclinic phase $Cu_2(OH)_2CO_3$. Fig. 4b shows that the morphology of the

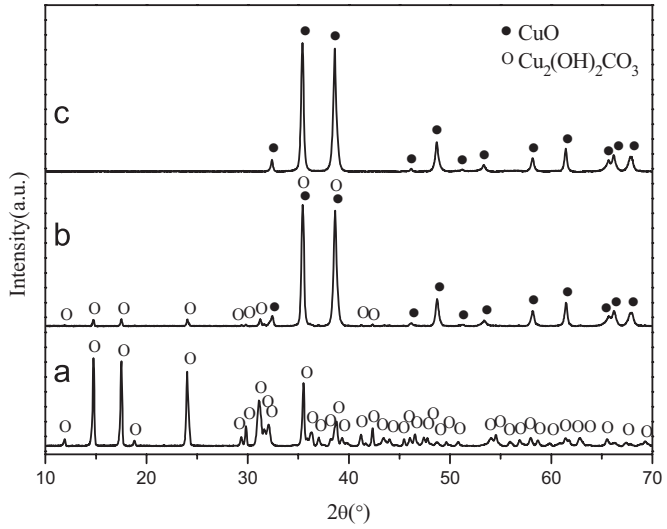

Fig. 1. XRD pattern of the products obtained at 180 °C in the presence of CTAB for different times: (a) 1 h, (b) 2 h, and (c) 6 h.

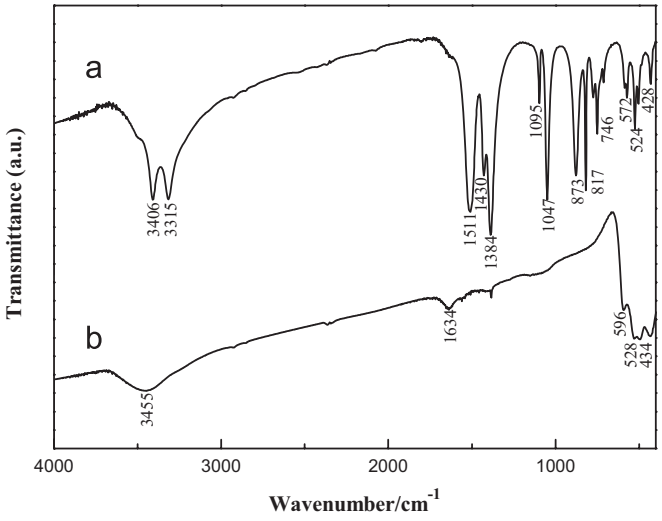

Fig. 2. FT-IR spectrum of the products obtained at 180 °C in the presence of CTAB for different times: (a) 1 h and (b) 6 h.

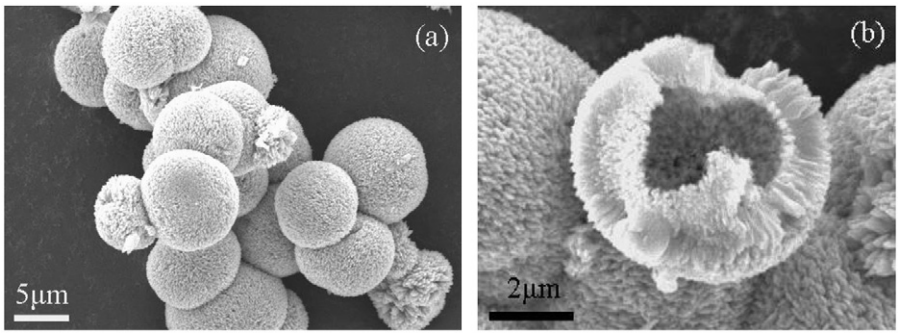

Fig. 3. (a, b) SEM images of the CuO obtained at 180 °C for 6 h in the presence of CTAB.

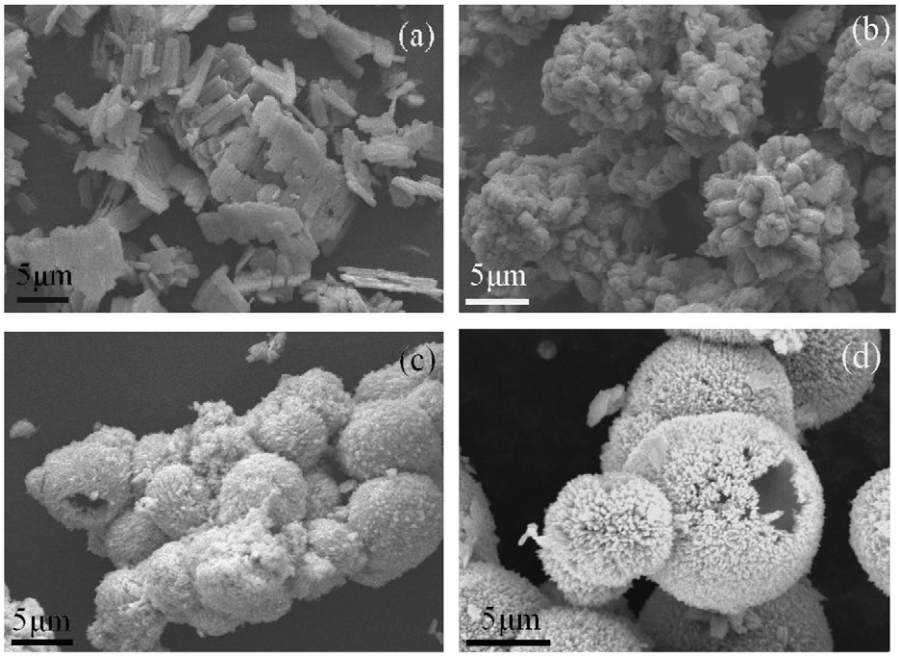

Fig. 4. SEM images of the products obtained at 180 °C in the presence of CTAB for different times: (a) 1 h, (b) 2 h, (c) 4 h, and (d) 6 h.

product is very similar to a cauliflower in shape, and the composition of this sample is a mixture of $Cu_2(OH)_2CO_3$ and CuO. Fig. 4c shows SEM image of CuO obtained by hydrothermal reaction for 4 h. The corresponding XRD results indicate that the hierarchical CuO were formed by decomposition of $Cu_2(OH)_2CO_3$. Fig. 4d shows SEM image of the dandelion-like CuO hollow microspheres obtained by hydrothermal reaction for 6 h.

3.2. Formation of the dandelion-like CuO hollow microspheres

Urea is a good precipitating agent because urea hydrolysis can provide both carbonate and hydroxyl anions slowly to form copper hydroxide carbonate [32]. Copper hydroxide carbonate may be decomposed to copper oxide by hydrothermal reaction at a high temperature. The main reaction in this system can be expressed as follows:

$$H_2NCONH_2 + H_2O \rightarrow 2NH_3 + CO_2, \quad (1)$$

$$CO_2 + H_2O \rightarrow {CO_3}^{2-} + 2H^+, \quad (2)$$

$$NH_3 + H_2O \rightarrow {NH_4}^+ + OH^-. \quad (3)$$

The formation of monoclinic copper hydroxide carbonate can be formulated as follows:

$$2Cu^{2+} + 2OH^- + {CO_3}^{2-} \leftrightarrow Cu_2(OH)_2CO_3. \quad (4)$$

The decomposition of copper hydroxide carbonate can be written as

$$Cu_2(OH)_2CO_3 \rightarrow 2CuO + H_2O + CO_2. \quad (5)$$

To investigate the growth process of the CuO hollow microspheres, time-dependent experiments were studied by hydrothermal reaction at 180 °C in the presence of CTAB. After the autoclave was heated for about 1 h, a green product precipitated out of the solution. The green product was composed of many tiny crystal strips (shown in Fig. 4a), and XRD results indicated that these strips were of monoclinic $Cu_2(OH)_2CO_3$ phase. Fig. 4b shows the SEM image of the product obtained for 2 h. The cauliflower product is mixture of $Cu_2(OH)_2CO_3$ and CuO (Figs. 1b and 4b). When the autoclave was heated for 4 h, CuO hollow microspheres were formed, and the morphologies were quite similar to those obtained in 6 h. The size of the $Cu_2(OH)_2CO_3$ crystal strips was bigger than the CuO crystal strips in the dandelion-like hollow microspheres (see Fig. 4), which may be attributed to the influence of reaction temperature on the growth and

decomposition of the $Cu_2(OH)_2CO_3$ crystal strips. When the reaction temperature was decreased to 140 °C even to 120 °C, both resulting products were of the $Cu_2(OH)_2CO_3$ phase (results not shown here, but are similar to those in Fig. 1a). Thus, bundles of $Cu_2(OH)_2CO_3$ tiny crystal strips were readily formed in a short reaction time (1 h, Fig. 4a) at a lower temperature. When the heating stopped, the reaction still continued, and the small crystal strips grew bigger during the cooling of the autoclave at an appropriate temperature (below 180 °C). Moreover, when the heating was maintained, the growth and decomposition of the $Cu_2(OH)_2CO_3$ crystal strips proceeded together at the temperature of 180 °C.

Based on the experimental results mentioned above, we proposed a formation mechanism for the dandelion-like CuO hollow microspheres in the presence of CTAB (Fig. 5). First, the tiny $Cu_2(OH)_2CO_3$ crystal strips are formed in a short time. Because there is an excessive amount of OH^- present in the solution, the $Cu_2(OH)_2CO_3$ is surrounded by OH^-, leading to the adsorption of OH^- onto the surface of $Cu_2(OH)_2CO_3$, resulting in the formation of $Cu_2(OH)_2CO_3 \cdot OH^-$ precursor [33]. Second, when the cationic CTAB template was added, electrostatic interactions between CTA^+ and negatively charges $Cu_2(OH)_2CO_3 \cdot OH^-$ induced the inorganic-surfactant complex formed. In this complex, $Cu_2(OH)_2CO_3 \cdot OH^-$ interact electrostatically with the positively charged surfactant cationic head group, CTA^+, to form a CTA^+–$Cu_2(OH)_2CO_3 \cdot OH^-$ ion pair [34]. The tiny $Cu_2(OH)_2CO_3$ crystal strips are assembled perpendicularly to the spherical surface, pointing toward the spherical CTA^+ micelles. Thus, the dandelion-like CuO hollow microspheres are formed during the decomposition of $Cu_2(OH)_2CO_3$ through a hydrothermal reaction at the temperature of 180 °C.

3.3. Other influences on the morphology of CuO hollow microspheres

The influence of other potential factors on the preparation of the dandelion-like CuO hollow microspheres was also studied. The molar ratio of Urea/Cu(Π) is a crucial factor on the formation of the hierarchical CuO hollow microspheres. When the molar ratio of Urea/Cu(Π) was less than 2:1, the products consisted of

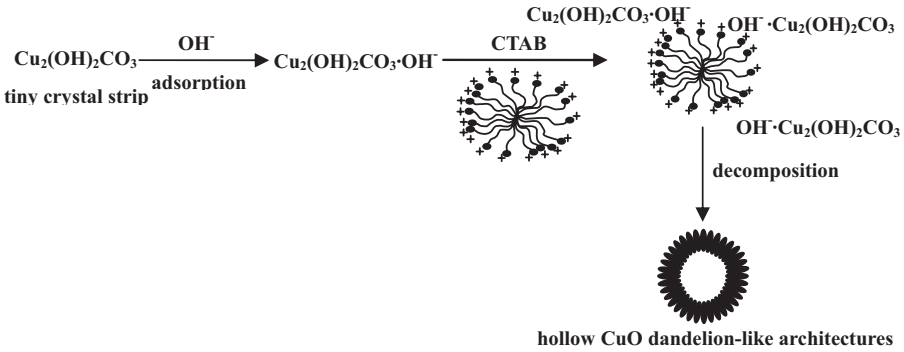

Fig. 5. The scheme for the formation of CuO hollow microspheres. Tiny $Cu_2(OH)_2CO_3$ crystal strips adsorbs OH^-, and become negative charged. Then, $Cu_2(OH)_2CO_3 \cdot OH^-$ binds to the cationic CTA^+ micelles, displaces Br^-, and the tiny $Cu_2(OH)_2CO_3$ crystal strips are assembled perpendicularly to the spherical surface, pointing toward the spherical CTA^+ micelles. Thus, the dandelion-like CuO hollow microspheres are formed due to the decomposition of $Cu_2(OH)_2CO_3$ through a hydrothermal reaction.

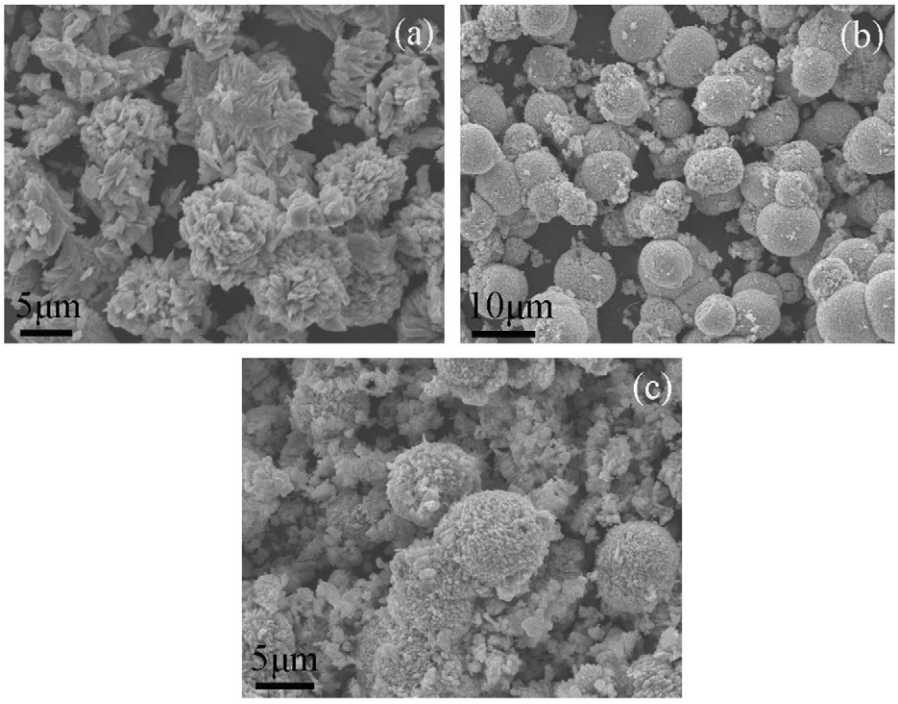

Fig. 6. SEM images of the products obtained at 180 °C in the presence of CTAB with the different molar ratio of Urea/Cu(Π): (a) 3:2, (b) 5:2, and (c) 10:2.

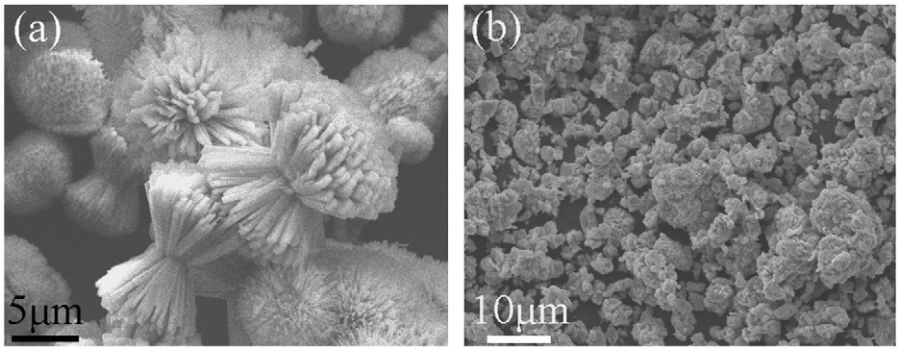

Fig. 7. SEM images of the products obtained at different temperature with no CTAB: (a) 100 °C and (b) 180 °C.

flower-shaped CuO with the full dimension of about 7–8 μm (Fig. 6a), while the molar ratio of Urea/Cu(Π) was greater than 4:1, the resulting products were a mixture of irregular microspheres and fragments (Fig. 6c). Thus, an appropriate molar ratio of Urea/Cu(Π) (2–4) may be favorable for the formation of the dandelion-like CuO hollow microspheres (Fig. 6b). A small quantity of OH^- existing in the solution may reduce the formation of $Cu_2(OH)_2CO_3 \cdot OH^-$, and the $Cu_2(OH)_2CO_3 \cdot OH^-$ is surrounded by CTA^+. During the nucleation and crystal growth processes, preferential adsorption between surfactant and the various crystallographic planes of the precursor could greatly reduce and/or enhance the growth rate along some directions [35,36]. Therefore, the flower-shaped CuO was formed by the selective adsorption between CTAB and certain crystal faces of CuO. When a large amount of OH^- ions are present in the solution, excess OH^- can shield the interaction between CTAB and $Cu_2(OH)_2CO_3 \cdot OH^-$, so that the interaction between these two species decreases, and the irregular microspheres and fragments were formed.

Moreover, under similar experimental conditions, the influence of other surfactants on the synthesis of the CuO hollow microspheres was also investigated. When polyvinylpyrrolidone (PVP) or sodium dodecylbenzene sulfonate (SDBS) was used as templates, or if no surfactant was utilized, no hollow microspheres could be formed. Only in the presence of CTAB were the uniform dandelion-like CuO hollow microspheres obtained. Otherwise, when the reaction temperature was decreased to 100 °C, many dandelion-like architectures of $Cu_2(OH)_2CO_3$ with monoclinic phase were obtained without CTAB (Fig. 7a). This phenomenon is similar to the formation of cobalt hydroxide carbonate [37]. Urea hydrolysis can provide both OH^- and CO_3^{2-}, which slowly deposit Cu^{2+} ion. Xu and Zeng [38] state that the CO_3^{2-} anions may act as an inhibitor that selectively decreases the rate of crystal growth in the direction of the side planes of the rod. Thus, the dandelion-like $Cu_2(OH)_2CO_3$ structures with no hollow interior were obtained at a lower temperature (about 100 °C). When the reaction temperature was increased to 180 °C, the reaction was too rapid to control the crystal growth without the assistance of CTAB. Therefore, the irregular CuO particles were obtained (Fig. 7b). It confirms that the reaction temperature and the CTAB surfactant both are crucial in the formation of the hierarchical CuO hollow microspheres.

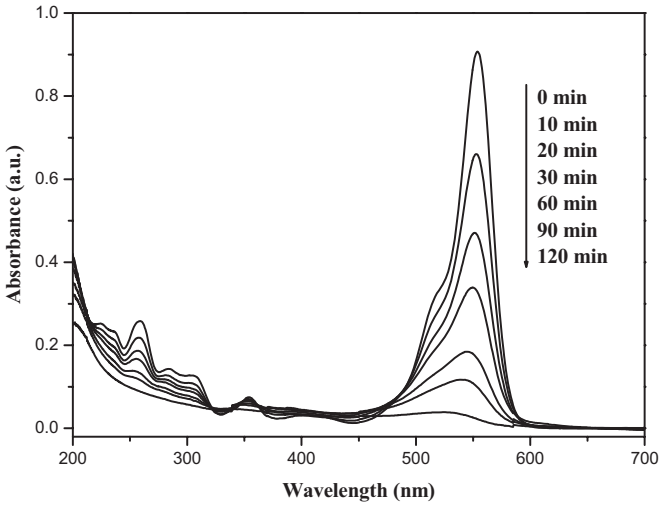

Fig. 8. Absorption spectrum of the RhB solution in the presence of dandelion-like CuO hollow microspheres under UV irradiation.

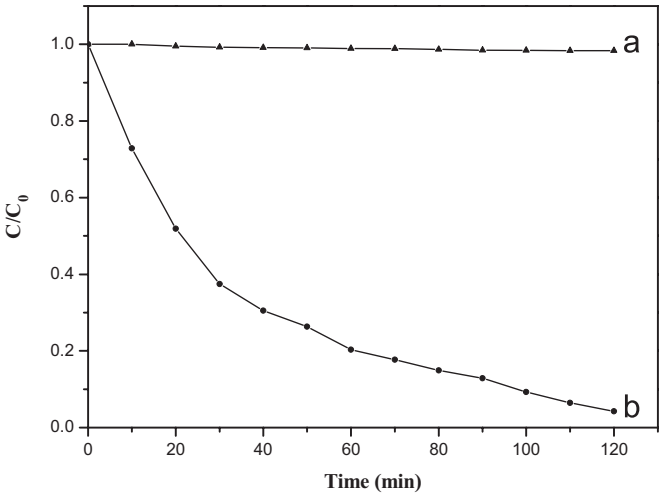

Fig. 9. Photodegradation of RhB (2.0×10^{-5} M, 20 mL) under UV-light: (a) no catalyst, (b) with 10 mg of dandelion-like CuO hollow microspheres. C is the concentration of RhB and C_o is the initial concentration.

3.4. Photocatalytic activity studies

Hollow CuO nanostructures, with a high specific surface area, can be utilized as catalysts for the decomposition of organic pollutants by the superoxides and/or hydroxyl radicals formed at the CuO interface [23]. To demonstrate the photocatalytic of the dandelion-like CuO hollow microspheres, the degradation of RhB was examined as a model reaction. The characteristic absorption of RhB at 553 nm was chosen to monitor the photocatalytic degradation process. Fig. 8 shows the UV–vis absorption spectrum of an aqueous solution of RhB (initial concentration: 2.0×10^{-5} M, 20 mL) in the presence of dandelion-like

CuO hollow microspheres (10 mg) under UV irradiation. The absorption peaks corresponding to RhB diminished gradually as the exposure time was extended. Significantly, Fig. 9 shows the concentration of RhB barely changed under the UV-light without the catalyst, which reveals the obvious photocatalytic ability of CuO. Due to the large surface area, more capacious interspaces of the dandelion-like CuO hollow architectures [39], and the recycling of Cu^{1+} ion under light on the CuO interface [23], photocatalyst can provide more active sites for the photocatalytic degradation of RhB molecules.

4. Conclusions

With the cationic surfactant CTAB as the template, dandelion-like CuO hollow microspheres have been successfully fabricated through a simple hydrothermal method. The reaction temperature, surfactant nature, and the molar ratio of Urea/Cu(II) all are crucial roles on the formation of the hierarchical CuO hollow microspheres. The dandelion-like CuO hollow microspheres exhibited a high photocatalytic activity for the photocatalytic decolorization of RhB aqueous solution under UV-light illumination. The unique hollow structures of the CuO microspheres may offer potential applications in areas such as catalysis, electronics, and optics.

Acknowledgments

This work was supported by the National Nature Science Foundation of China (Grant nos. 50672088 and 60571029).

References

[1] J.A. Switaer, H.M. Kothari, P. Poizot, S. Nakanishi, E.W. Bohannan, Nature 425 (2003) 490–493.
[2] A. Chowdhuri, V. Gupta, K. Sreenivas, R. Kumar, S. Mozumdar, P.K. Patanjali, Appl. Phys. Lett. 84 (2004) 1180–1183.
[3] X.P. Gao, J.L. Bao, G.L. Pan, H.Y. Zhu, P.X. Huang, F. Wu, D.Y. Song, J. Phys. Chem. B 108 (2004) 5547–5551.
[4] W.J. Dong, X. Li, L. Shang, Y.Y. Zheng, G. Wang, C.R. Li, Nanotechnology 20 (2009) 035601.
[5] P.C. Dai, H.A. Mook, G. Aeppli, S.M. Hayden, F. Dogan, Nature 406 (2000) 965–968.
[6] C. Li, X.G. Yang, B.J. Yang, Y. Yan, Y.T. Qian, Eur. J. Inorg. Chem. 19 (2003) 3534–3537.
[7] X.M. Sun, J.F. Liu, Y.D. Li, Chem. Eur. J. 12 (2006) 2039–2047.
[8] F. Caruso, Chem. Eur. J. 6 (2000) 413–419.
[9] J.X. Huang, Y. Xie, B. Li, Y. Liu, Y.T. Qian, S.Y. Zhang, Adv. Mater. 12 (2000) 808–811.
[10] Y.D. Yin, R.M. Rioux, C.K. Erdonmez, S. Hughes, G.A. Somorjai, A.P. Alivisatos, Science 304 (2004) 711–714.
[11] H.J. Fan, M. Knez, R. Scholz, K. Nielsch, E. Pippel, D. Hesse, M. Zacharias, U. Gösele, Nat. Mater. 5 (2006) 627–631.
[12] H.G. Yang, H.C. Zeng, J. Phys. Chem. B 108 (2004) 3492–3495.
[13] H.C. Zeng, J. Mater. Chem. 16 (2006) 649–662.
[14] J.G. Yu, H.T. Guo, S.A. Davis, S. Mann, Adv. Funct. Mater. 16 (2006) 2035–2041.
[15] J.G. Yu, H.G. Yu, H.T. Guo, M. Li, S. Mann, Small 4 (2008) 87–91.
[16] B. Liu, H.C. Zeng, J. Am. Chem. Soc. 126 (2004) 8124–8125.
[17] Y.G. Zhang, S.T. Wang, Y.T. Qian, Z.D. Zhang, Solid State Sci. 8 (2006) 462–466.
[18] H.G. Yu, J.G. Yu, S.W. Liu, S. Mann, Chem. Mater. 19 (2007) 4327–4334.
[19] C.H.B. Ng, W.Y. Fan, J. Phys. Chem. C 111 (2007) 9166–9171.
[20] J.Q. Qi, H.Y. Tian, L.T. Li, H.L.W. Chan, Nanoscale Res. Lett. 2 (2007) 107–111.
[21] Z.L. Jin, X.J. Zhang, Y.X. Li, S.B. Li, G.X. Lu, Catal. Commun. 8 (2007) 1267–1273.
[22] H.Z. Ma, Q.F. Zhuo, B. Wang, Environ. Sci. Technol. 41 (2007) 7491–7496.
[23] J. Bandara, I. Guasaquillo, P. Bowen, L. Soare, W.F. Jardim, J. Kiwi, Langmuir 21 (2005) 8554–8559.
[24] T.J. Yan, X.X. Wang, J.L. Long, P. Liu, X.L. Fu, G.Y. Zhang, X.Z. Fu, J. Colloid Interface Sci. 325 (2008) 425–431.
[25] N.R. Jana, L. Gearheart, C.J. Murphy, Chem. Commun. (2001) 617–618.
[26] J. Yao, W. Tjandra, Y.Z. Chen, K.C. Tam, J. Ma, B. Soh, J. Mater. Chem. 13 (2003) 3053–3057.
[27] R. Zielinski, S. Ikeda, H. Nomura, S. Kato, J. Colloid Interface Sci. 125 (1988) 497–507.
[28] J.G. Yu, X.F. Zhao, B. Cheng, Q.J. Zhang, J. Solid State Chem. 178 (2005) 861–867.
[29] M. Yang, G. Wang, Z.Z. Yang, Mater. Chem. Phys. 111 (2008) 5–8.
[30] L.F. Hu, Z.L. Tang, Z.T. Zhang, Microporous Mesoporous Mater. 113 (2008) 41–46.
[31] R.A. Nyquist, R.O. Kagel, Infrared Spectra of Inorganic Compounds, Academic Press, New York, London, 1971, p. 9.
[32] Z.G. Zhao, F.X. Geng, J.B. Bai, H.M. Cheng, J. Phys. Chem. C 111 (2007) 3848–3852.
[33] Y. Yu, F.P. Du, J.C. Yu, Y.Y. Zhuang, P.K. Wong, J. Solid State Chem. 177 (2004) 4640–4647.
[34] J. Perez-Juste, L.M. Liz-Marzan, S. Carnie, D.Y.C. Chan, P. Mulvaney, Adv. Funct. Mater. 14 (2004) 571–579.
[35] Y.G. Sun, B. Mayers, T. Herricks, Y.N. Xia, Nano Lett. 3 (2003) 955–960.
[36] J.G. Yu, X.F. Zhao, B. Cheng, Q.J. Zhang, J. Solid State Chem. 178 (2005) 861–867.
[37] B.X. Li, Y. Xie, C.Z. Wu, Z.Q. Li, J. Zhang, Mater. Chem. Phys. 99 (2006) 479–486.
[38] R. Xu, H.C. Zeng, J. Phys. Chem. B 107 (2003) 12643–12649.
[39] B.X. Li, Y. Xie, M. Jing, G.X. Rong, Y.C. Tang, G.Z. Zhang, Langmuir 22 (2006) 9380–9385.